Apoptosis 2005; **10**: 895–907
© *2005 Springer Science + Business Media, Inc. Manufactured in The Netherlands.*

Ornithine decarboxylase prevents methotrexate-induced apoptosis by reducing intracellular reactive oxygen species production

C.-C. Huang, P.-C. Hsu, Y.-C. Hung, Y.-F. Liao, C.-C. Liu, C.-T. Hour, M.-C. Kao, G.J. Tsay, H.-C. Hung* and G.-Y. Liu*

Tzu Hui Institute of Technology, Pingtung, Taiwan, R.O.C (C.-C. Huang); Department of Medicine, Da-Chien General Hospital, Miao-Li, Taiwan, R.O.C (P.-C. Hsu); Institute of Immunology, Chung Shan Medical University, Taichung, Taiwan, R.O.C (Y.-C. Hung, C.-C. Liu, G.-Y. Liu); Institute of Biochemistry, Kaohsiung Medical University, Kaohsiung, Taiwan, R.O.C (C.-T. Hour); Department of Life Sciences, National Chung-Hsing University, Taichung, Taiwan, R.O.C (Y.-F. Liao, H.-C. Hung); School of Medical, China Medical University, Taichung, Taiwan, R.O.C (M.-C. Kao); Department of Internal Medicine, Chung Shan Medical University Hospital, Taichung, Taiwan, R.O.C. (G.J. Tsay)

Methotrexate (MTX), a folate antagonist, was developed for the treatment of malignancies, and is currently used in rheumatoid arthritis (RA) and other chronic inflammatory disorders. It has been proven in short-term and long-term prospective studies that low doses of MTX (0.75 mg/Kg/week) are effective in controlling the inflammatory manifestations of RA. Low-concentrations of MTX achieve apoptosis and clonal deletion of activated peripheral T cells. One of the mechanisms of the anti-inflammatory and immunosuppressive effects may be the production of reactive oxygen species (ROS). However, the drug resistance of MTX in malignancies remains poorly understood. Ornithine decarboxylase (ODC) plays an important role in diverse biological functions, including cell development, differentiation, transformation, growth and apoptosis. In our previous studies, ODC overexpression was shown to prevent TNFα-induced apoptosis via reducing ROS. Here, we also investigated one mechanism of MTX-induced apoptosis and of drug resistance as to the anti-apoptotic effects of ODC during MTX treatment. We found MTX could induce caspase-dependent apoptosis and promote ROS generation together with disrupting the mitochondrial membrane potential ($\Delta\Psi_m$) of HL-60 and Jurkat T cells. Putrescine and ROS scavengers could reduce MTX-induced apoptosis, which leads to the loss of $\Delta\Psi_m$, through reducing intracellular ROS. Overexpression of ODC in parental cells had the same effects as putrescine and the ROS scavengers. Moreover, ODC overexpression prevented the decline of Bcl-2 that maintains $\Delta\Psi_m$, the cytochrome c release and activations of caspase 9 and 3 following MTX treatment. The results demonstrate that MTX-induced apoptosis is ROS-dependent and occurs along a mitochondria-mediated pathway. Overexpressed ODC cells are resistant to MTX-induced apoptosis by reducing intracellular ROS production.

Keywords: apoptosis; caspase; methotrexate; ODC; ROS.

Abbreviations: MTX, methotrexate; ODC, ornithine decarboxylase; ROS, reactive oxygen species; $\Delta\Psi_m$, mitochondrial membrane potential; DFMO, difluoromethylornithine; DCFH-DA, 2′,7′-dichlorofluorescin diacetate; z-VAD-fmk, benzyloxycarbonyl-Val-Ala-Asp-fluoromethyl ketone.

Introduction

Methotrexate (MTX), the 4-amino, 10-methyl analogue of folic acid, is the most widely used antifolate against many malignancies in cancer chemotherapy, including leukemia, breast cancer, colorectal cancer, head and neck cancer, lymophma, osteogenic sarcoma, urothelial cancer, and choriocarcinoma. It is also used in the treatment of nonmalignant disorders, such as psoriasis, rheumatoid arthritis and graft-versus-host diseases.[1] Clinically, high doses of MTX cause tumor shrinkage.[2–4] High doses of MTX induce apoptosis in several cell lines, including Chinese hamster ovary cells,[5,6] human leukemic T lymphocytes such as CCRF-CEM and Jurkat T cells,[6,7] hepatoma cell lines[8] and keratinocytes.[9] Low doses of MTX also induce apoptosis of mitogen-activated $CD4^+$ and $CD8^+$ T cells, but not resting T cells. Furthermore, low doses of MTX lead to clonal deletion of activated T cells in mixed lymphocyte reactions.[10,11]

There are several mechanisms by which MTX-induced apoptosis have been investigated. MTX can induce the production of reactive oxygen species (ROS) and apoptosis

*Correspondence to: Prof. Guang-Yaw Liu, Institute of Immunology, Chung-Shan Medical University, No. 110, Sec. 1, Chien-Kuo N. Road, Taichung, Taiwan, ROC. Tel: (886)-4-2473-0022 (ext. 11709); Fax: (886)-4-23248172; e-mail: liugy@csmu.edu.tw and Prof. Hui-Chih Hung, Department of Life Sciences, National Chung-Hsing, University, No. 250, Kuo-Kuang Road, Taichung, Taiwan, ROC. Tel: (886)-4-2284-0416 (ext. 505); Fax: (886)-4-22851856; e-mail: hchung@dragon.nchu.edu.tw

in Jurkat T cells via ROS.[12] Overexpression of Bcl-2 results in increased resistance to cell destruction by MTX,[13] and down-regulation of bcl-2 by synthetic bcl-2 antisense oligonucleotides resulting in a marked enhancement in the sensitivity of tumor cells to chemotherapeutic drugs.[14] Bcl-2 is a protein anchored in the membrane of the mitochondria. It maintains mitochondrial membrane potential ($\Delta\Psi_m$) by protecting apoptosis from any attacks. It seems that mitochondria-mediated apoptotic pathway play a role in MTX-induced apoptosis. In addition, MTX activates specific caspases and induces apoptosis, which are blocked by zVAD-fluoromethyl ketone, a general caspase inhibitor.[15] Therefore, the caspase pathway may also play a role in this process.

Ornithine decarboxylase (ODC, EC 4.1.1.17), the first and rate-limiting enzyme of the polyamine biosynthetic pathway, decarboxylates L-ornithine to form putrescine.[16] ODC and polyamines (putrescine, spermidine and spermine) play an important role in several biological functions, including embryonic development, the cell cycle and proliferation,[17] and in the origin and progression of neoplastic diseases.[18,19] The polyamine pathway is an important target of therapeutic intervention in many cancers.[17] Polyamine deprivation enhances the efficacy of chemotherapy.[20] Measurement of ODC activity is useful in predicting the chemosensitivity to many anti-cancer drugs including MTX.[21] ODC and polyamines have paradoxical roles in preventing or enhancing apoptosis during different cell insults or cell lines.[17] Inhibition of ODC activity by DFMO can induce apoptosis of HC11 mouse mammary epithelial cells, which is associated with a rapid increase in ROS concentration.[22] Moreover, overexpression of ODC promotes survival of human gastric cancer cells under stressful conditions, such as H_2O_2, radiation and some chemotherapeutic drugs including cisplatin, doxorubicin, paclitaxel, 5-flourouracil.[23] The purpose of the present study was to investigate whether ODC could prevent MTX-induced apoptosis. In addition, we aimed to determine exactly how and by what mechanism ODC prevented MTX-induced apoptosis.

Materials and methods

Chemicals and cell culture

MTX, ribonuclease A (RNase A), N-acetylcysteine (NAC), catalase, vitamin C, putrescine, benzyloxycarbonyl-Val-Ala-Asp-fluoromethyl ketone (z-VAD-fmk), acridine orange, propidium iodide (PI), 2′, 7′-dichlorofluorescin diacetate (DCFH-DA), rhodamine 123 and HA14-1 were purchased from Sigma (St Louis, MO). The human promyelocytic leukemia HL-60 cells and Jurkat T cells were grown in 90% RPMI 1640 and 10% FBS (fetal bovine serum) obtained from Gibco BRL (Grand Island, NY) at a temperature of 37°C under a humidified, 5% CO_2 atmosphere.

Cell viability and acridine-orange staining

Cell numbers were counted using trypan blue exclusion assay. Morphological change and cell viability were detected by light microscopic observation. To identify apoptotic character upon MTX stimulation, 5×10^4 cells in 10 μl cell suspension were mixed with an equal volume of acridine orange solution (10 μg/ml) in phosphate-buffered saline (PBS) on each slide. Green fluorescence was detected by microscope as being between 500–525 nm (Olympus America, St Huntington, NY).[24]

Cloning of human ODC and cell transfection

Parental cells were grown in RPMI 1640 medium supplemented with 10% heat-inactivated FBS for 3 h, and then the harvested cells were gently rinsed in PBS. Purification of mRNA was carried out according to the supplier's instructions (Mdbio, Taiwan) and the cDNA was synthesized by reverse transcriptase (Promega, Madison, WI). Polymerase chain reaction (PCR) amplification of the encoding region of the human ODC cDNA was performed with our designed primers derived from the human ODC sequence. The PCR product was sequenced and sub-cloned to eukaryotic expression vector, pCMV-Tag (Novagen, Madison, WI). The plasmid of ODC expression was constructed by inserting the *Bam*HI-*Eco*RI 1,415 bp coding region fragment. Parental cells were transfected with WT-ODC (overexpressing ODC), m-ODC (frameshift mutant) and DN-ODC (dominant-negative ODC) plasmids according to calcium phosphate-mediated transfections, respectively.[25] Stably transfected cells were selected with the antibiotic G418 (400 μg/ml). After approximately 3 weeks, G418-resistant clones were isolated and analyzed individually for expression of ornithine decarboxylase. The individual clones were examined for expression of ODC by RT-PCR, immunoblotting and enzyme activity assays. Overexpressed Bcl-2 cells were built as previously described.[26]

Site-directed mutagenesis of *odc* gene

To construct dominant-negative ODC (K69A/C360A-ODC; DN-ODC), site-directed mutagenesis was performed as described previously.[27] WT-ODC plasmid and two pairs of synthetic oligonucleotide primers containing the desired mutations (point mutations to alanine at lysine 69 [K69A] and cysteine 360 [C360A] residues) were utilized and *in vitro* site-directed mutagenesis was

performed using *pfu* DNA polymerase (Promega) following the instructions from the manufacturer.

DNA fragmentation analysis

For this, 5×10^6 cells were harvested in PBS and lysed overnight in a digestion buffer (0.5% sarkosyl, 0.5 mg/ml proteinase K, 50 mM Tris-HCl, pH 8.0 and 10 mM EDTA) at 55°C. Subsequently cells were treated with 0.5 μg/ml RNase A for 2 h. The genomic DNA was extracted by phenol-chloroform-isoamyl alcohol extraction and analyzed by gel electrophoresis at 50 volts for 90 min using 2% agarose. Approximately 20 μg of genomic DNA was loaded in each well, visualized under ultraviolet (UV) light and photographed.

ODC enzyme activity assay

ODC enzyme activity was assayed at 37°C through measuring its product and putrescine as described previously[28] with the following modification. Samples were suspended in ODC buffer (50 μM EDTA, 25 μM pyridoxal phosphate and 2.5 mM DTT in 25 mM Tris HCl, pH 7.1) incubated with 2 nmole of L-ornithine for 1 h, and the material was then spotted onto p81 phosphocellulose (Whatman, Maidstone, England). Diamines were eluted from the dried papers by shaking at 37°C for 60 min with 0.5 ml quantities of elution buffer (0.5 M magnesium chloride in 0.2 M boric acid-borax buffer, pH 8.4). Following this, samples were supplemented by 400 μl of luminescence reagent (11.7 μg/ml luminal, 30 μg/ml peroxidase type II (EC 1.11.1.7) and 67 mM glycine buffer, pH 8.6 (at 1:1:2.5, v/v/v) to each cuvette. By retaining the cuvettes in the dark for 30 min, the background was able to measure using a TR 717 microplate luminometer (Perkin-Elmer, Foster, CA). Then 5 μl of diamine oxidase (4.61 $\mu g/\mu l$) (Sigma) were injected into each cuvette, and luminescence was recorded for 40 sec at 37°C with the results being calculated according to the standard curve using putrescine.

Apoptotic sub-G1 analysis

For this, 1×10^6 cells were cultured in 35-mm petri dishes and incubated for 24 h. Cells were treated with MTX for time course and dose-dependence, then harvested and washed with PBS, resuspended in 0.2 ml of PBS, fixed in 0.8 ml of ice-cold 100% ethanol at −20°C overnight. The cell pellets were collected by centrifugation, resuspended in 1 ml of hypotonic buffer (0.5% Triton X-100 in PBS and 0.5 μg/ml RNase), and incubated at 37°C for 30 min. Then, 1 ml of PI solution (50 μg/ml) was added and the mixture was allowed to stand on ice for 30 min. The nuclei were analyzed in a FACSCAN laser flow cytometer (Becton Dickenson, San Jose, CA).

Detection of intracellular reactive oxygen species (ROS)

Intracellular oxidative stress was assayed by measuring intracellular oxidation of 2′, 7′-dichlorofluorescin (DCFH).[29,30] The resulting substrate is DCFH-DA, which easily diffuses into the cell and is then deacetylated by cellular esterases to the more hydrophilic, nonfluorescent DCFH. ROS generation in the cell oxidizes DCFH to the fluorescent 2′, 7′-dichlorofluorescein (DCF). DCF fluorescence was measured in a flow cytometer using the Cell Quest software (Becton Dickenson). In each study, 10000 events (cells) were counted. The results were presented as a percentage of the fluorescence intensity compared with the control sample.

Detection of mitochondrial membrane potential ($\Delta\Psi_m$)

Mitochondrial potential was monitored by fluorescence of rhodamine 123.[31,32] Incubation was continued for 10 min with 10 μM rhodamine 123. Finally, the cells were detached and fluorescence was measured in a flow cytometer. In each study, 10000 events (cells) were counted. Data were acquired and analyzed with Cell Quest software.

Immunoblotting

Mitochondrial and cytosolic proteins were isolated from cells after treatment with 1 μM MTX for 24 h, as previously described.[33] In order to extract mitochondrial proteins, cell (5×10^6) pellets were washed once with ice-cold PBS and resuspended with 50 μl of mitochondrial buffer (25 mM Tris, pH 6.8, 1 mM EDTA, 1 mM DTT, 0.1 mM PMSF and 250 mM sucrose). To purify the total proteins, cells were harvested and lysed in cold lysis buffer (10% v/v glycerol, 1% v/v Triton X-100, 1 mM sodium orthovanadate, 1 mM EGTA, 10 mM NaF, 1 mM sodium pyrophosphate, 20 mM Tris, pH 7.9, 100 μM β-glycerophosphate, 137 mM NaCl, 5 mM EDTA, 1 mM PMSF, 10 μg/ml aprotinin and 10 μg/ml leupoptin), homogenized, centrifuged, and the supernatant was boiled in a loading buffer with an aliquot corresponding to 50 μg of protein being separated by SDS-PAGE. After blotting, the membranes were incubated with anti-cytochrome c, anti-Bcl-2, anti-caspase 3, anti-caspase 9, anti-Apaf-1, anti-PARP and anti-α-tubulin antibodies (Santa Cruz, Santa Cruz, CA) for 6 h and the second

antibody labeled with horseradish-peroxidase was incubated for 1 h. The antigen-antibody complexes were visualized by the enhanced chemiluminescence (Amersham Pharmacia Biotech, Piscataway, NJ).

Results

MTX induced caspase-dependent apoptosis, ROS generation and the loss of mitochondrial membrane potential ($\Delta\Psi_m$)

We first investigated the cell death induced by MTX. HL-60 and Jurkat T cells were treated with 0, 0.1, 0.5, 1 and 10 μM of MTX with or without zVAD-fmk, a total caspase inhibitor, for 24 h. Cells were observed by fluorescence-microscope and the percentage of apoptosis was recorded. We found MTX could induce apoptosis in a dose-dependent manner (Figure 1A). The morphologic changes were chromatin condensation, membrane blebbing and shrinkage, and apoptotic body formation. Then, cells were harvested for DNA gel electrophoresis and flow cytometry with propidium iodide (PI) staining. Furthermore, there was a time course as indicated and dose-dependent increases in DNA fragmentation after MTX treatment. We found zVAD-fmk (500 nM, pretreated for 1 h before MTX) could block this phenomenon

Figure 1. MTX induced caspase-dependent apoptosis in HL-60 and Jurkat T cells. HL-60 and Jurkat T cells were treated with MTX 0, 0.1, 0.5, 1 or 10 μM for the indicated times after having been treated with or without zVAD-fmk (500 nM) for 1 h. (A) HL-60 and Jurkat T cells were observed by fluorescence-microscope and counted for their percentage of apoptosis. (B) HL-60 cells were assayed by DNA fragmentation, microscope and flow cytometry with propidium iodide (PI) staining. The arrow indicates an apoptotic body. M, DNA ladder marker.

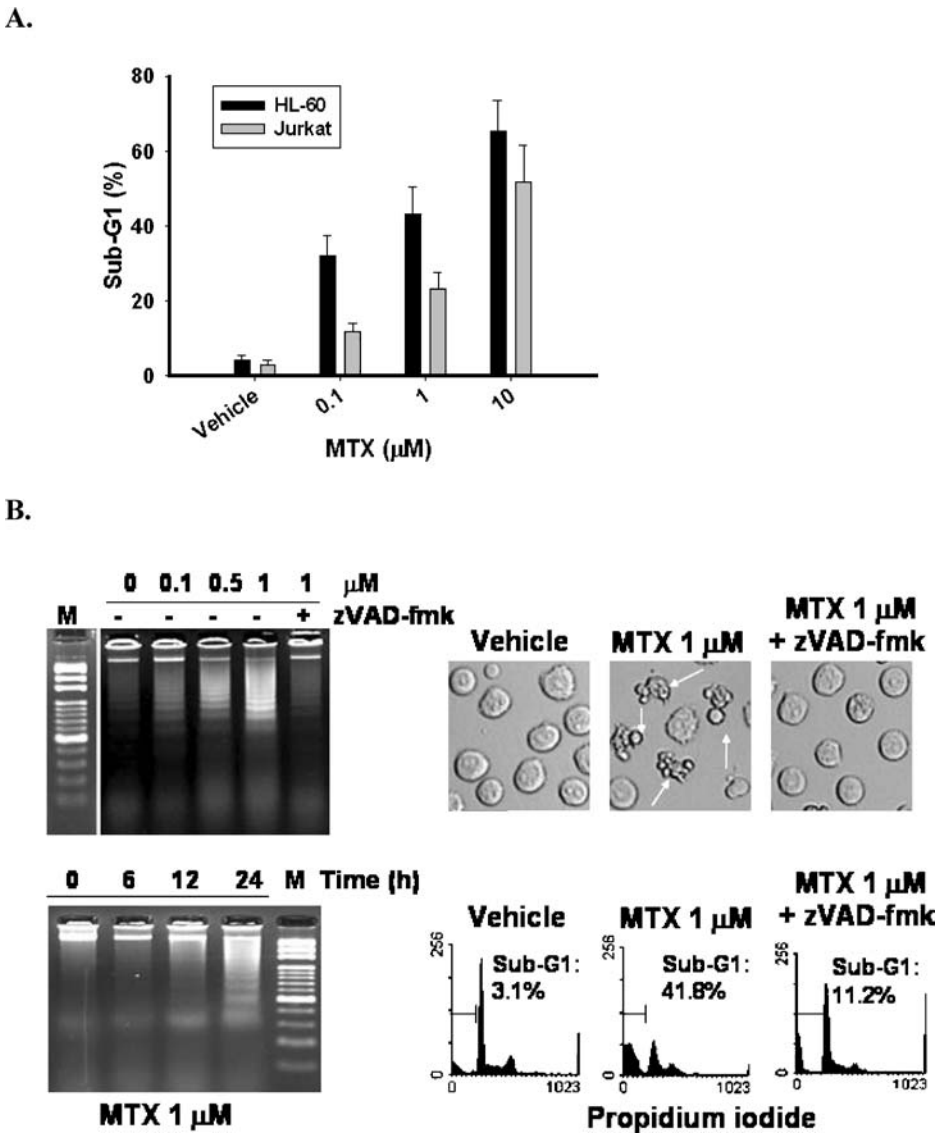

(Figure 1B). For the experiment of flow cytometry with PI staining, the sub-G1 peak ratios were 3.1%, 41.8% and 11.2% in cells treated with vehicle, MTX (1 μM) and MTX combined with zVAD-fmk, respectively. zVAD-fmk could decrease the sub-G1 peak ratio after MTX treatment up to 82%. All of the aforementioned morphologic and molecular changes are features typical of apoptosis.[34] As shown in a previous study,[15] MTX-induced apoptosis could be blocked by z-VAD-fmk. All these data indicated that MTX could induce caspase-dependent apoptosis.

In order to measure intracellular ROS, HL-60 cells were treated with 0, 0.1, 0.5 and 1 μM MTX for 1 h and then incubated with 5 μM DCFH-DA after MTX treatment at 37°C. Intracellular ROS was quantified by flow cytometry, using a permeable cell fluorescent probe DCFH-DA. DCFH-DA is hydrolyzed by intracellular esterases to nonfluorescent 2′, 7′-dichlorofluorescin (DCFH), which is rapidly oxidized by ROS to generate the fluorescent 2′, 7′-dichlorofluorescein (DCF). DCF is very useful in quantifying overall oxidative stress in cells.[35,36] To assess $\Delta\Psi_m$, rhodamine 123,[31] a green fluorescent mitochondrial dye, was measured by flow cytometry after MTX treatment for 24 h. The results of flow cytometric analysis showed there were dose-dependent increases of intracellular ROS generation and dose-dependent decreases of $\Delta\Psi_m$ in HL-60 cells after MTX treatment (Figure 2). These results indicated that MTX-induced apoptosis was coupled by the generation of ROS and the loss of $\Delta\Psi_m$.

Putrescine and ROS scavengers could reduce MTX-induced apoptosis and the loss of $\Delta\Psi_m$ by reducing intracellular ROS

To clarify the role of ROS in the mechanism of MTX-induced apoptosis and the effects of putrescine, we pretreated 1 mM putrescine and 10 mM NAC for 3 h. Other ROS scavengers, such as catalase (100 U) and vitamin C (1 mM) were pretreated for 1 h prior to 1 μM MTX treatment. After MTX treatment for 24 h, all of the cells were observed by fluorescence-microscope. We found MTX could induce apoptotic morphologic changes, including chromatin condensation, membrane blebbing and shrinkage, and apoptotic body formation. However, these apoptotic morphologic changes occurred less if cells were pretreated with ROS scavengers or putrescine (data not shown). In the flow cytometric assay with PI fluorescence, we found that putrescine, vitamin C, NAC and catalase decreased the sub-G1 peak ratio following MTX treatment. However, inhibition of the endogenous ODC activity with DFMO increased the sensitivity to MTX-induced apoptosis (Figure 3). Among these ROS scavengers, catalase was the most effective. It reduced the sub-G1 ratio by up to 55% and putrescine decreased the ratio by about 50% as compared with the vehicle.

Intracellular ROS and $\Delta\Psi_m$ were determined by measuring DCF after treatment for 1 h and rhodamine 123 after treatment for 24 h with flow cytometry, respectively. Putrescine and NAC were shown to be capable of significantly decreasing intracellular ROS and maintaining

Figure 2. MTX caused increasing intracellular ROS and the loss of mitochondrial membrane potential ($\Delta\Psi_m$). HL-60 cells were treated with MTX 0, 0.1, 0.5 or 1 μM. Intracellular ROS and $\Delta\Psi_m$ were detected by flow cytometry by measuring the fluorescence of DCF (1 h) and rhodamine 123 (24 h), respectively. Cells were treated with H_2O as a vehicle control. The production of ROS and $\Delta\Psi_m$ are expressed as the percentage of fluorescent cells in contrast with the control cells. Data are representative of at least three experiments.

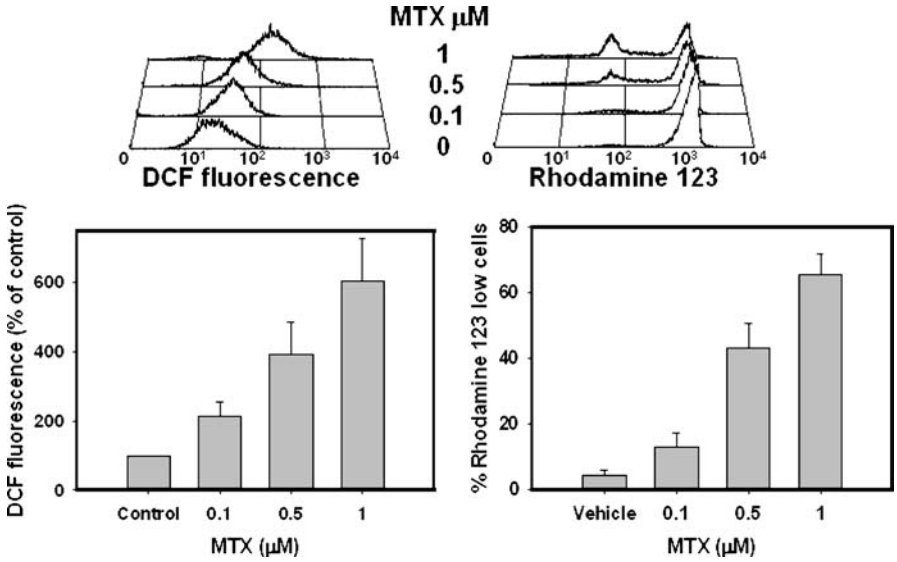

Figure 3. Putrescine and ROS scavengers reduced MTX-induced apoptosis. HL-60 cells were pretreated with NAC (10 mM), putrescine (1 mM) or DFMO (1 mM) for 3 h, pretreated with vitamin C (1 mM) or catalase (100 U) for 1 h before MTX (1 μM) treatment. After MTX treatment for 24 h, the sub-G1 peak ratio was measured by flow cytometry with PI fluorescence. Data are representative of at least three experiments. Cells were treated with H_2O as a vehicle control. Vit C, vitamin C.

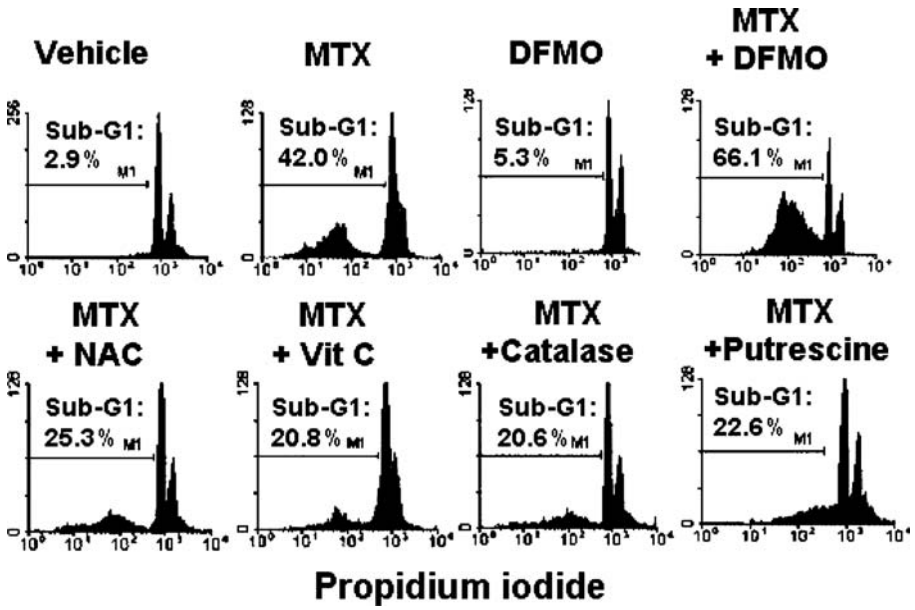

$\Delta\Psi_m$ after MTX treatment (Figure 4). Putrescine and ROS scavengers could prevent more than half of cells from undergoing apoptosis. Taken together, these results indicate MTX-induced apoptosis occurs mainly through the ROS-dependent pathway. Putrescine exerts a protective effect in MTX-induced apoptosis via decreasing intracellular ROS and maintaining the $\Delta\Psi_m$.

ODC overexpression could reduce intracellular ROS and prevent MTX-induced loss of $\Delta\Psi_m$ and apoptosis

We further examined the role of ODC in MTX-induced apoptosis. We constructed ODC cDNA into a system of mammalian expression plasmid, pCMV-Tag and generated cell lines overexpressing ODC in parental HL-60 and Jurkat T cells, named WT-ODC and JK-WT-ODC cells, respectively. Parental HL-60 and Jurkat T cells were transfected by its frame-shift mutant vector as a control, which were termed m-ODC and JK-m-ODC cells, respectively. At the same time, we also used the method of site-directed mutagenesis to construct dominant-negative ODC and build DN-ODC cells.[37] ODC was overexpressed in WT-ODC cells at the transcriptional and translational level, respectively (data not shown). Four hours after being stimulated by 10% FBS in parental HL-60, m-ODC, WT-ODC and DN-ODC cells treated with or without 1 mM DFMO, WT-ODC cell expressed about two folds greater ODC enzyme activity than parental HL-60 and m-ODC cells. This overexpression of ODC activity could be significantly inhibited by DFMO (Figure 5). In addition, intracellular ROS had decreased more in WT-ODC cells than in m-ODC significantly after 10% FBS stimulation for 4 h (Figure 6A). One hour after MTX (1 μM) treatment in the m-ODC and WT-ODC cells, significantly more intracellular ROS had accumulated in the m-ODC cells than in the WT-ODC cells (Figure 6B) This result revealed that ODC overexpression reduced intracellular ROS whether MTX induction had taken place or not. Twenty-four hours after MTX treatment, WT-ODC was more resistant to MTX-induced apoptosis than parental HL-60, m-ODC and DN-ODC cells in experiments of phase light microscopy (data not shown) and flow cytometry with PI staining. The percentage of apoptotic sub-G1 in WT-ODC cells had decreased by approximately 20 and 34% as compared with total parental HL-60 cells subjected to 1 μM MTX treatment for 24 h and parental Jurkat T cells treated by 10 μM MTX for 48 h, respectively (Figure 6C and D). The protective effect of ODC in WT-ODC cells was reversed by DMFO (Figure 6E). In the experiment involving $\Delta\Psi_m$, WT-ODC cells had significantly less loss of $\Delta\Psi_m$ than parental HL-60, m-ODC and DN-DOC cells. In addition, DFMO, inhibiting the activity of ODC, blocked the maintaining of $\Delta\Psi_m$ in WT-ODC cells (Figure 7A). MTX also induced the disruption of $\Delta\Psi_m$ and apoptosis in JK-m-ODC cells. It achieved a similar level of disruption for the HL-60 cell system, but less for JK-WT-ODC cells (Figure 7B). Furthermore, WT-ODC cells prevented cytochrome c release from mitochondria to

Figure 4. Putrescine reduced intracellular ROS and the loss of $\Delta\Psi_m$ after MTX treatment, as ROS scavengers. HL-60 cells were pretreated with NAC (10 mM) or putrescine (1 mM) for 3 h before MTX (1 mM) treatment. Intracellular ROS and $\Delta\Psi_m$ were detected by flow cytometry with measuring fluorescence of DCF (A) and rhodamine 123 (B), respectively. Data are representative of at least three experiments. * $P < 0.05$ as compared to HL-60 cell only treated MTX. Put, putrescine.

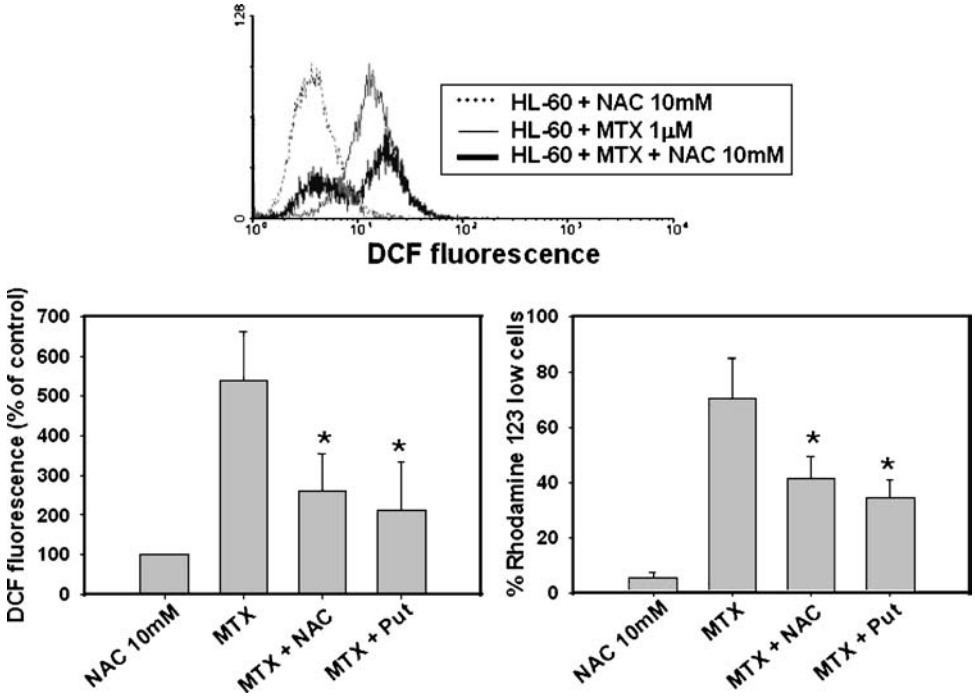

Figure 5. ODC overexpression increased ODC activity, which was reversed by DFMO. Parental HL-60, wild-type ODC (WT-ODC), frame-shift mutant ODC (m-ODC) and dominant-negative ODC (DN-ODC) cells were stimulated by 10% FBS with or without 1 mM DFMO. ODC enzyme activity was measured after 4 h of stimulation. Data are representative of at least three experiments. * $P < 0.05$, ** $P < 0.01$ and *** $P < 0.001$.

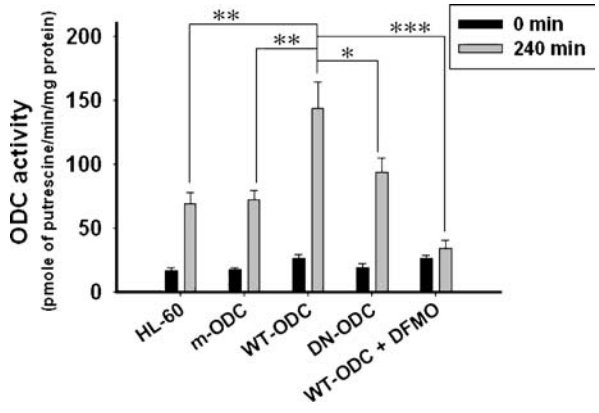

cytosol after MTX treatment (Figure 7C). Based on these data, MTX-induced apoptosis seemed to occur through the mitochondria-mediated pathway. ODC overexpression reduced ROS accumulation, and disrupted $\Delta\Psi_m$ and cytochrome c release after being induced by MTX. Simultaneously, ODC overexpression reduced at least a part of the apoptosis following MTX treatment of the HL-60 and Jurkat T cell systems.

ODC overexpression prevented the decline of Bcl-2 that maintained $\Delta\Psi_m$ and reduced MTX-induced apoptosis

Following stimulation by 10% FBS, m-ODC, WT-ODC and DN-ODC cells were treated with or without MTX. ODC overexpression could efficiently prevent the decline of Bcl-2 following MTX untreatment (1.4 folds) and treatment (3 folds), respectively (Figure 8A). In addition, Bcl-2 inhibitor (HA14-1) enhanced the disruption of $\Delta\Psi_m$ and apoptosis of WT-ODC cells after MTX treatment (data not shown). It was revealed that the mitochondria-mediated pathway perhaps plays an important role in MTX-induced apoptosis. Bcl-2 can maintain $\Delta\Psi_m$, avoid cytochrome c release from the mitochondria and prevent apoptosis.[38] In previous studies, Bcl-2 overexpression was found to prevent MTX-induced apoptosis.[39,40] To confirm the importance of the mitochondria-mediated pathway in MTX-induced apoptosis, we transfected the *bcl-2* gene (Bcl-2 cells) or its vector alone (vector cells) into parental HL-60 cells.[26] Bcl-2 cells and vector cells were treated with or without MTX, and then harvested for flow cytometry with rhodamine 123 and PI staining. We

Figure 6. ODC overexpression reduced the intracellular ROS and MTX-induced ROS generation and apoptosis. After being stimulated by 10% FBS for 0 or 4 h, m-ODC and WT-ODC cells were harvested for flow cytometry with measuring fluorescence of DCF (A). m-ODC and WT-ODC cells were treated with or without MTX (1 μM) for 1 h, and then intracellular ROS was measured by flow cytometry (B). Parental, m-ODC, WT-ODC and DN-ODC cells were treated with or without MTX after 1 mM DFMO treatment or not for 3 h. Sub-G1 peak ratio was measured by flow cytometry with PI staining in HL-60 (C) and Jurkat T cells (D), respectively. Cells were observed and counted for the percentage of apoptosis by phase-construct microscope (E). Data are representative of at least three experiments. * $P < 0.05$, as compared to parental HL-60 or m-ODC cells.

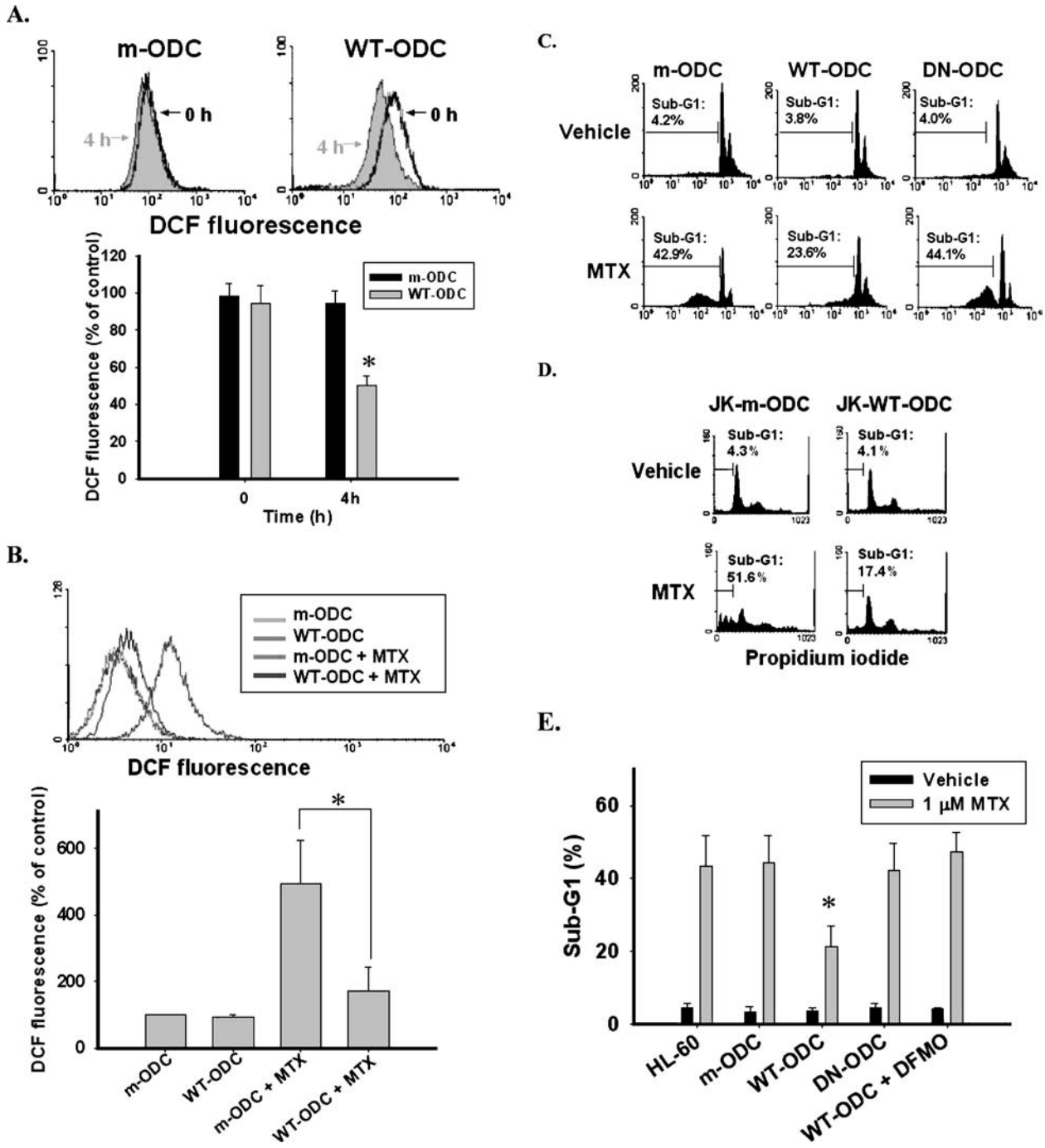

Figure 7. ODC overexpression reduced the loss of $\Delta\Psi_m$ and cytochrome c release. After being stimulated by 10% FBS, parental HL-60, m-ODC, WT-ODC and DN-ODC cells were treated with or without MTX (1 μM) for 24 h after treated DFMO or not. $\Delta\Psi_m$ was measured by flow cytometry with rhodamine 123 (A). The $\Delta\Psi_m$ of JK-m-ODC and JK-WT-ODC cells were detected by flow cytometry with rhodamine 123 (B). Cytoplasmic and mitochondrial proteins were separated and detected by immunoblotting with cytochrome c antibody (C).

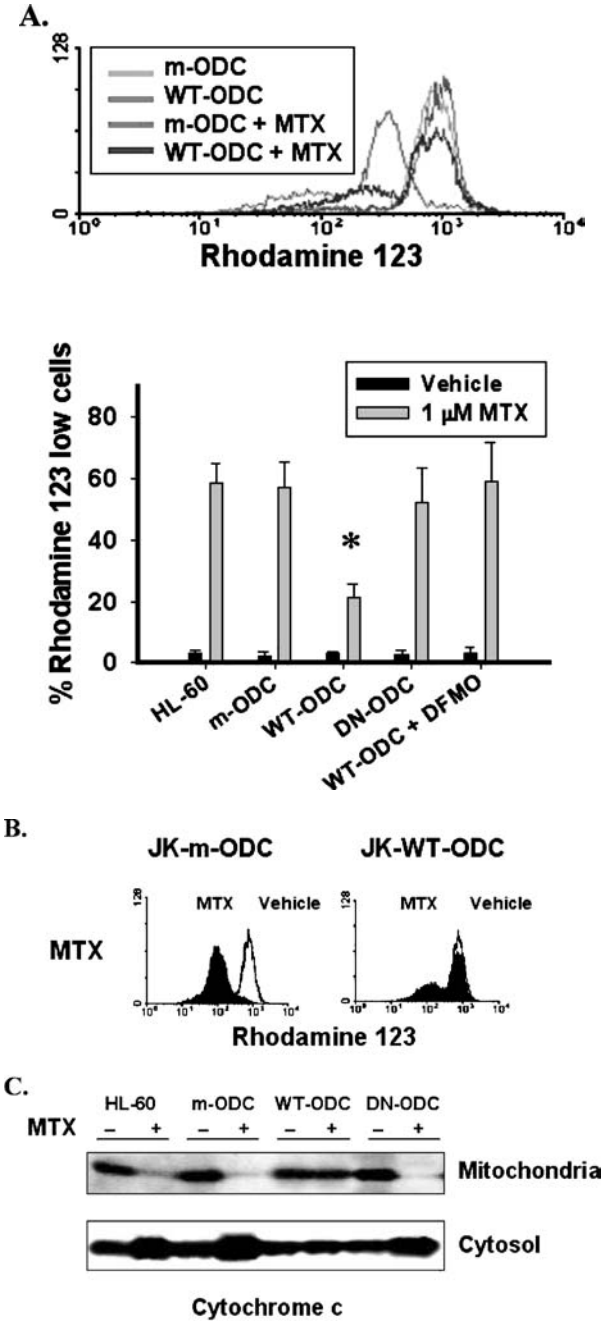

found Bcl-2 cells had lost less $\Delta\Psi_m$ and sub-G1 peak ratio than their vector cells (Figure 8B and C). Indeed, our data revealed that ODC overexpression prevented the decline of Bcl-2 and Bcl-2 overexpression in parental

Figure 8. ODC overexpression prevented the decline of Bcl-2 which maintained $\Delta\Psi_m$ and reduced MTX-induced apoptosis. After being stimulated by 10% FBS, m-ODC, WT-ODC and DN-ODC cells were treated with or without MTX (1 μM) for 24 h and total proteins were analyzed by immunoblotting with Bcl-2 and a-tubulin antibody (A). Parental HL-60 and overexpression of Bcl-2 cells were treated with and without MTX. Cells were harvested for measuring $\Delta\Psi_m$ (B) and sub-G1 peak ratio (C) by flow cytometry with rhodamine 123 and PI fluorescence, respectively. Data are representative of at least three experiments.

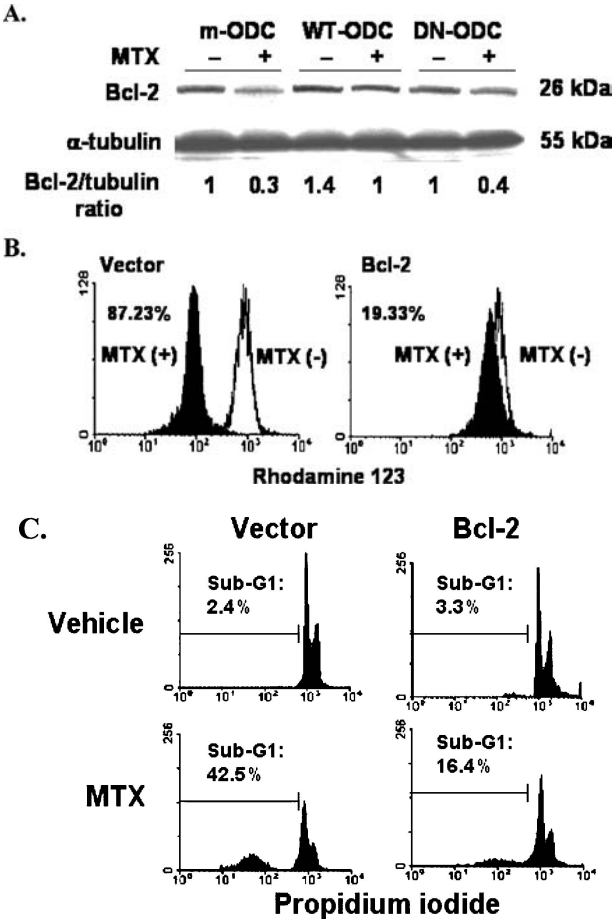

HL-60 cells decreasing the disruption of $\Delta\Psi_m$ and apoptosis induced by MTX. Therefore, maintaining $\Delta\Psi_m$ through the use of ROS scavengers, putrescine, ODC overexpression and Bcl-2 in parental cells are ways of preventing MTX-induced apoptosis.

ODC overexpression prevented the activation of caspase 9, 3 and the formation of apoptosome after MTX treatment

According to the above results, cytochrome c was released after MTX treatment in parental HL-60, m-ODC and DN-ODC cells, but to a lesser extent in WT-ODC cells. In addition, MTX-induced apoptosis in HL-60 cells seemed to occur mainly through the

Figure 9. ODC overexpression prevented the cleavage of caspase 9, 3 and PARP and the generation of Apaf-1. After being stimulated by 10% FBS for 3 h, m-ODC, WT-ODC and DN-ODC cells were treated with or without MTX (1 μM) for 24 h. Total protein were extracted for immunoblotting with antibodies of caspase 9, Apaf-1, caspase 3 and PARP. Data are representative of at least three experiments.

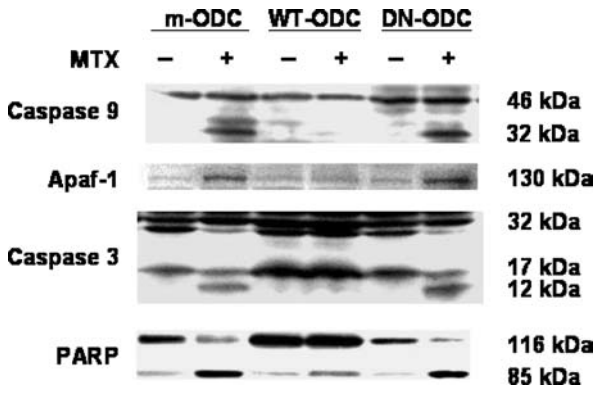

mitochondria-mediated pathway. To clarify the downstream of the ODC-involved mitochondria-mediated pathway after MTX-induced apoptosis, m-ODC, WT-ODC and DN-ODC cells were treated with or without MTX. Total proteins from diverse cells were detected by immunoblotting with anti-Apaf-1, caspase 9, 3 and PARP (the substrate of caspase 3). In the WT-ODC cells, we found that Apaf-1 had decreased, the activation of caspase 9 and 3 were inhibited, and the cleavage of PARP was significantly more protected as compared with the m-ODC and DN-ODC cells after MTX treatment (Figure 9). The results indicated that ODC overexpression prevented the formation of apoptosome (the complex of Apaf-1, cytochrome c and caspase 9) and inhibited the activation of caspase 3 cascade during apoptotic progression.

Discussion

When cells are treated by MTX, extracellular MTX is transported into cells through at least two different energy-dependent mechanisms. One is a relatively low-affinity reduced folate transmembrane carrier in the micromolar range and the other is a membrane-associated folate-binding protein with nanomolar affinity. Intracellular MTX is converted to polyglutamate forms by the binding of two to five of the polyglutamate groups, resulting in an increase in its intracellular half-life. MTX and its polyglutamate derivatives inhibit dihydrofolate reductase (DHFR), the major MTX target, and several folate-dependent enzymes such as thymidylate synthase (TS) and 5-amino-imidazole-4-carboxamide ribonucleotide (AICAR) transformaylase.[41]

The main pharmacological action of MTX is its inhibition of these enzymes during thymidine and purine synthesis.[42–45] Purine and pyrimidine nucleotides play critical roles in DNA and RNA synthesis as well as in membrane lipid biosynthesis and protein glycosylation. They are necessary for the development and survival of mature T lymphocytes. Pyrimidines control progression from early to intermediate S phase in the cell cycle. Inhibition of pyrimidine synthesis by MTX is a way of inducing apoptosis of activated T lymphocytes.[10,46] There are several reports demonstrating that apoptosis caused by anticancer drugs, including MTX, may be mediated via the CD95 system.[6] MTX-induced apoptosis may proceed via expression of CD95-L and ligation of the death receptor CD95 in leukemia T cell lines and hepatoma, gastric cancer, colon cancer, and breast cancer cell lines.[6,8,47] However, in activated human peripheral blood T-lymphocytes (PBL), MTX triggers apoptosis via a CD95-independent pathway.[10] Here, we demonstrate another novel mechanism of MTX-induced apoptosis. That is, MTX induces caspase-dependent apoptosis in HL-60 and Jurkat T cells in a time- and dose-dependent manner. After MTX treatment, intracellular ROS accumulates in the initial one hour and $\Delta\Psi_m$ loss is detected 24 h later. ROS scavenges, such as NAC, vitamin C and catalase, could reduce the accumulation of intracellular ROS, prevent loss of $\Delta\Psi_m$, and protect at least part of the cells from apoptosis. These data provide evidence that MTX causes $\Delta\Psi_m$ disruption and apoptosis in HL-60 and Jurkat T cells via ROS generation. Overexpression of Bcl-2 also prevents MTX-induced disruption of $\Delta\Psi_m$ and apoptosis. Furthermore, apoptosome formation, activation of caspase 3 and cleavage of PARP (substrate of caspase 3) are found after MTX treatment. There is evidence to suggest that the mitochondria-mediated pathway participates in MTX-induced apoptosis.

How can MTX induce the generation of ROS? One possible mechanism is that MTX inhibits the activity of enzymes involved in enzyme defense mechanisms against ROS, including glucose-6-phosphate dehydrogenase, glucose-6-phosphogluconate dehydrogenase, glutathione reductase and gamma-glutamylcysteine synthetase. High doses of MTX decrease the cellular levels of glutathione and reduce the effectiveness of the antioxidant enzyme defense system.[48] It has been demonstrated that glutathione depletion induces ROS generation and disrupts $\Delta\Psi_m$, resulting in mitochondrial cytochrome c release, caspase 3 activation, DNA fragmentation and finally apoptosis.[49] In another study, MTX increased the amount of hydrogen peroxide released by stimulated polymorphonuclear neutrophils (PMNs) in a dose-dependent manner.[50] Low doses of MTX also induced a time- and dose-dependent increase in cytosolic peroxide in U937 monocytes and Jurkat T cells. ROS generation by MTX is important for cytostasis in monocytes and cytotoxicity T cells.[12] Our results confirm previous studies and also show

that one of the mechanisms of MTX-induced apoptosis is through a ROS-dependent, mitochondria-mediated pathway.

It is known that overexpression of ODC can prevent cells from apoptosis for many insults, including H_2O_2, radiation and some chemotherapeutic drugs including cisplatin, doxorubicin, paclitaxel, 5-flourouracil.[23] We provide the evidence that putrescine or overexpression of ODC can prevent MTX-induced apoptosis. Furthermore, treatment with putrescine or overexpression of ODC in HL-60 and Jurkat T cells can decrease intracellular ROS without MTX treatment and reduce the accumulation of ROS following the addition of MTX. Putrescine and overexpression of ODC also maintain $\Delta\Psi_m$ and prevent apoptosis following the performance of MTX treatment as a ROS scavenger, such as NAC, vitamin C, and catalase. These protective effects of ODC are not seen in DN-ODC cells and are blocked by DFMO. Through the mitochondria-mediated apoptotic pathway, WT-ODC prevented the formation of apoptosome and cytochrome c release from mitochondria to cytosol. Moreover, it inhibited the activation of caspase 3 and the cleavage of PARP (the substrate of caspase 3). A previous study suggested that the inherent ROS level might be determinative in tumor cells as to their apoptotic susceptibility to As_2O_3.[51] Overexpression of ODC seems to reinforce the ability of the anti-oxidant defense system to decrease the inherent ROS level and enhance the resistance of tumor cells to anti-cancer drugs.

Furthermore, how can putrescine and ODC reduce ROS *in vivo*? Overexpression of ODC or treatment with putrescine in cells increases the concentration of polyamines. Spermine, one of the polyamines, can function directly as a free radical scavenger.[52] Inhibition of ODC by DFMO could increase intracellular ROS, and might lead to an imbalance in polyamine pools. Polyamine catabolism by polyamine oxidase (PAO) could continue and result in the production of ROS.[53] MTX also inhibits the synthesis of spermidine and spermine in stimulated lymphocytes for patients with rheumatoid arthritis through inhibition of the SAM-dependent pathway.[54] Thus, overexpression of ODC possibly reduces ROS generation during polyamine catabolism, and overcomes the inhibitory effects of MTX on the polyamine biosynthetic pathway.

In conclusion, low doses of MTX induce apoptosis of HL-60 and Jurkat T cells in a time- and dose-dependent manner. MTX-induced apoptosis occurs via ROS-dependent and mitochondria-mediated pathways in at least part of the cells. Putrescine and overexpression of ODC can maintain $\Delta\Psi_m$, avoiding cytochrome c release and the formation of apoptosome. This inhibits the activation of caspase 3 and prevents apoptosis, functioning as ROS scavengers. Our results explain why ODC activity affects the chemosensitivity of anti-cancer drugs and supports the suggestion that ODC is an important target for chemotherapeutic intervention in the combined treatment of cancers.

Acknowledgments

This study was supported by the grants from the National Science Council NSC 93-2320-B-040-048 and NSC 93-2745-B-040-005-URD, and by the Chung Shan Medical University grant CSMU 93-OM-A-104.

References

1. DeVita VT, Hellman S, Rosenberg SA. Principles & Practice of Oncology. In: *Cancer*. Lippincott Williams & Wilkins 2001: 388.
2. Meyers PA, Gorlick R, Heller G, *et al*. Intensification of preoperative chemotherapy for osteogenic sarcoma: results of the Memorial Sloan-Kettering (T12) protocol. *J Clin Oncol* 1998; **16**: 2452–2458.
3. Silverman LB, McLean TW, Gelber RD, *et al.* Intensified therapy for infants with acute lymphoblastic leukemia: results from the Dana-Farber Cancer Institute Consortium. *Cancer* 1997; **80**: 2285–2295.
4. Williams SF, Gilewski T, Mick R, Bitran JD. High-dose consolidation therapy with autologous stem-cell rescue in stage IV breast cancer: follow-up report. *J Clin Oncol* 1992; **10**: 1743–1747.
5. Barry MA, Behnke CA, Eastman A. Activation of programmed cell death (apoptosis) by cisplatin, other anticancer drugs, toxins and hyperthermia. *Biochem Pharmacol* 1990; **40**: 2353–2362.
6. Friesen C, Herr I, Krammer PH, Debatin KM. Involvement of the CD95 (APO-1/FAS) receptor/ligand system in drug-induced apoptosis in leukemia cells. *Nat Med* 1996; **2**: 574–577.
7. da Silva CP, de Oliveira CR, da Conceicao M, de Lima P. Apoptosis as a mechanism of cell death induced by different chemotherapeutic drugs in human leukemic T-lymphocytes. *Biochem Pharmacol* 1996; **51**: 1331–1340.
8. Muller M, Strand S, Hug H, *et al*. Drug-induced apoptosis in hepatoma cells is mediated by the CD95 (APO-1/Fas) receptor/ligand system and involves activation of wild-type p53. *J Clin Invest* 1997; **99**: 403–413.
9. Heenen M, Laporte M, Noel JC, de Graef C. Methotrexate induces apoptotic cell death in human keratinocytes. *Arch Dermatol Res* 1998; **290**: 240–245.
10. Genestier L, Paillot R, Fournel S, Ferraro C, Miossec P, Revillard JP. Immunosuppressive properties of methotrexate: apoptosis and clonal deletion of activated peripheral T cells. *J Clin Invest* 1998; **102**: 322–328.
11. Paillot R, Genestier L, Fournel S, Ferraro C, Miossec P, Revillard JP. Activation-dependent lymphocyte apoptosis induced by methotrexate. *Transplant Proc* 1998; **30**: 2348–2350.
12. Phillips DC, Woollard KJ, Griffiths HR. The anti-inflammatory actions of methotrexate are critically dependent upon the production of reactive oxygen species. *Br J Pharmacol* 2003; **138**: 501–511.
13. Miyashita T, Reed JC. bcl-2 gene transfer increases relative resistance of S49.1 and WEHI7.2 lymphoid cells to cell death and DNA fragmentation induced by glucocorticoids and

multiple chemotherapeutic drugs. *Cancer Res* 1992; **52**: 5407–5411.
14. Kitada S, Takayama S, De Riel K, Tanaka S, Reed JC. Reversal of chemoresistance of lymphoma cells by antisense-mediated reduction of bcl-2 gene expression. *Antisense Res Dev* 1994; 4: 71–79.
15. Papaconstantinou HT, Xie C, Zhang W, *et al.* The role of caspases in methotrexate-induced gastrointestinal toxicity. *Surgery* 2001; **130**: 859–865.
16. Tabor CW, Tabor H. Polyamines. *Annu Rev Biochem* 1984; **53**: 749–790.
17. Thomas T, Thomas TJ. Polyamines in cell growth and cell death: molecular mechanisms and therapeutic applications. *Cell Mol Life Sci* 2001; **58**: 244–258.
18. Moshier JA, Dosescu J, Skunca M, Luk GD. Transformation of NIH/3T3 cells by ornithine decarboxylase overexpression. *Cancer Res* 1993; **53**: 2618–2622.
19. Auvinen M, Laine A, Paasinen-Sohns A, *et al*. Human ornithine decarboxylase-overproducing NIH3T3 cells induce rapidly growing, highly vascularized tumors in nude mice. *Cancer Res* 1997; 57: 3016–3025.
20. Quemener V, Moulinoux JP, Havouis R, Seiler N. Polyamine deprivation enhances antitumoral efficacy of chemotherapy. *Anticancer Res* 1992; **12**: 1447–1453.
21. Bachrach U, Shayovitz A, Marom Y, Ramu A, Ramu N. Ornithine decarboxylase—a predictor for tumor chemosensitivity. *Cell Mol Biol (Noisy-le-grand)* 1994; **40**: 957–964.
22. Ploszaj T, Motyl T, Zimowska W, Skierski J, Zwierzchowski L. Inhibition of ornithine decarboxylase by alpha-difluoromethylornithine induces apoptosis of HC11 mouse mammary epithelial cells. *Amino Acids* 2000; **19**: 483–496.
23. Park JK, Chung YM, Kang S, *et al*. c-Myc exerts a protective function through ornithine decarboxylase against cellular insults. *Mol Pharmacol* 2002; **62**: 1400–1408.
24. Liu GY, Chen KJ, Lin-Shiau SY, Lin JK. Peroxyacetyl nitrate-induced apoptosis through generation of reactive oxygen species in HL-60 cells. *Mol Carcinog* 1999; **25**: 196–206.
25. Kao MC, Liu GY, Chuang TC, Lin YS, Wuu JA, Law SL. The N-terminal 178-amino-acid domain only of the SV40 large T antigen acts as a transforming suppressor of the HER-2/neu oncogene. *Oncogene* 1998; **16**: 547–554.
26. Hour TC, Chen L, Lin JK. Suppression of transcription factor NF-kappaB activity by Bcl-2 protein in NIH3T3 cells: implication of a novel NF-kappaB p50-Bcl-2 complex for the anti-apoptotic function of Bcl-2. *Eur J Cell Biol* 2000; **79**: 121–129.
27. Kunkel TA. Rapid and efficient site-specific mutagenesis without phenotypic selection. *Proc Natl Acad Sci USA* 1985; **82**: 488–492.
28. Wang Y, Bachrach U. A luminescence-based test for determining ornithine decarboxylase activity. *Anal Biochem* 2000; **287**: 299–302.
29. Amer J, Goldfarb A, Fibach E. Flow cytometric measurement of reactive oxygen species production by normal and thalassaemic red blood cells. *Eur J Haematol* 2003; **70**: 84–90.
30. Carter WO, Narayanan PK, Robinson JP. Intracellular hydrogen peroxide and superoxide anion detection in endothelial cells. *J Leukoc Biol* 1994; **55**: 253–258.
31. Juan G, Cavazzoni M, Saez GT, O'Connor JE. A fast kinetic method for assessing mitochondrial membrane potential in isolated hepatocytes with rhodamine 123 and flow cytometry. *Cytometry* 1994; **15**: 335–342.
32. Davis S, Weiss MJ, Wong JR, Lampidis TJ, Chen LB. Mitochondrial and plasma membrane potentials cause unusual accumulation and retention of rhodamine 123 by human breast adenocarcinoma-derived MCF-7 cells. *J Biol Chem* 1985; **260**: 13844–13850.
33. McConkey DJ, Lin Y, Nutt LK, Ozel HZ, Newman RA. Cardiac glycosides stimulate Ca2+ increases and apoptosis in androgen-independent, metastatic human prostate adenocarcinoma cells. *Cancer Res* 2000; **60**: 3807–3812.
34. Kerr JF, Wyllie AH, Currie AR. Apoptosis: A basic biological phenomenon with wide-ranging implications in tissue kinetics. *Br J Cancer* 1972; **26**: 239–257.
35. Wang H, Joseph JA. Quantifying cellular oxidative stress by dichlorofluorescein assay using microplate reader. *Free Radic Biol Med* 1999; **27**: 612–616.
36. Ubezio P, Civoli F. Flow cytometric detection of hydrogen peroxide production induced by doxorubicin in cancer cells. *Free Radic Biol Med* 1994; **16**: 509–516.
37. Shantz LM, Guo Y, Sawicki JA, Pegg AE, O'Brien TG. Overexpression of a dominant-negative ornithine decarboxylase in mouse skin: effect on enzyme activity and papilloma formation. *Carcinogenesis* 2002; **23**: 657–664.
38. Hockenbery DM, Oltvai ZN, Yin XM, Milliman CL, Korsmeyer SJ. Bcl-2 functions in an antioxidant pathway to prevent apoptosis. *Cell* 1993; **75**: 241–251.
39. Miyashita T, Reed JC. Bcl-2 oncoprotein blocks chemotherapy-induced apoptosis in a human leukemia cell line. *Blood* 1993; **81**: 151–157.
40. Simonian PL, Grillot DA, Nunez G. Bcl-2 and Bcl-XL can differentially block chemotherapy-induced cell death. *Blood* 1997; **90**: 1208–1216.
41. Genestier L, Paillot R, Quemeneur L, Izeradjene K, Revillard JP. Mechanisms of action of methotrexate. *Immunopharmacology* 2000; **47**: 247–257.
42. Bertino JR. Karnofsky memorial lecture. Ode to methotrexate. *J Clin Oncol* 1993; **11**: 5–14.
43. Bertino JR, Goker E. Drug resistance in acute leukemia. *Leuk Lymphoma* 1993; **11**: 37–41.
44. Chabner BA. The evolution of cancer chemotherapy. *Hosp Pract (Off Ed)* 1985; **20**: 115–119, 123–127.
45. Chabner BA, Allegra CJ, Curt GA, *et al*. Polyglutamation of methotrexate. Is methotrexate a prodrug? *J Clin Invest* 1985; **76**: 907–912.
46. Quemeneur L, Gerland LM, Flacher M, Ffrench M, Revillard JP, Genestier L. Differential control of cell cycle, proliferation, and survival of primary T lymphocytes by purine and pyrimidine nucleotides. *J Immunol* 2003; **170**: 4986–4995.
47. Muller M, Wilder S, Bannasch D, *et al*. p53 activates the CD95 (APO-1/Fas) gene in response to DNA damage by anticancer drugs. *J Exp Med* 1998; **188**: 2033–2045.
48. Babiak RM, Campello AP, Carnieri EG, Oliveira MB. Methotrexate: Pentose cycle and oxidative stress. *Cell Biochem Funct* 1998; **16**: 283–293.
49. Armstrong JS, Jones DP. Glutathione depletion enforces the mitochondrial permeability transition and causes cell death in Bcl-2 overexpressing HL60 cells. *Faseb J* 2002; **16**: 1263–1265.
50. Gressier B, Lebegue S, Brunet C, *et al*. Pro-oxidant properties of methotrexate: evaluation and prevention by an anti-oxidant drug. *Pharmazie* 1994; **49**: 679–681.
51. Yi J, Gao F, Shi G, *et al*. The inherent cellular level of reactive oxygen species: One of the mechanisms determining apoptotic

susceptibility of leukemic cells to arsenic trioxide. *Apoptosis* 2002; 7: 209–215.
52. Ha HC, Sirisoma NS, Kuppusamy P, Zweier JL, Woster PM, Casero RA. Jr. The natural polyamine spermine functions directly as a free radical scavenger. *Proc Natl Acad Sci USA* 1998; **95**: 11140–11145.
53. Morgan DM. Polyamines. An overview. *Mol Biotechnol* 1999; **11**: 229–250.
54. Nesher G, Osborn TG, Moore TL. *In vitro* effects of methotrexate on polyamine levels in lymphocytes from rheumatoid arthritis patients. *Clin Exp Rheumatol* 1996; 14: 395–399.